

The complete modulational instability gain spectrum of nonlinear QPM gratings

Joel F. Corney

Department of Physics, University of Queensland, St. Lucia Qld 4072, Australia

Ole Bang

Research Centre COM, Technical University of Denmark, DK-2800 Kongens Lyngby, Denmark

We consider plane waves propagating in quadratic nonlinear slab waveguides with nonlinear quasi-phase-matching gratings. We predict analytically and verify numerically the complete gain spectrum for transverse modulational instability, including hitherto undescribed higher order gain bands.

OCIS codes: 190.4410, 190.4420

I. INTRODUCTION

With the maturing of the quasi-phase-matching (QPM) technique, in particular by electric-field poling of ferro-electric materials, such as LiNbO_3 [1], by poling of polymers [2] and quantum-well disordering in semiconductors [3], the number of applications of quadratic nonlinear (or $\chi^{(2)}$) materials has increased significantly. Even complicated QPM grating structures are now commercially available in periodically poled LiNbO_3 (PPLN). It is therefore more important than ever to have complete knowledge of the effects a QPM grating has on the properties of $\chi^{(2)}$ materials. The most fundamental effect of a QPM grating, with a certain spectrum of spatial wave vectors, is to allow noncritical phase matching at all wavelengths for which the wave-vector mismatch Δk matches a component of the grating spectrum. Thus QPM gratings allow for efficient multiple wavelength second harmonic generation (SHG) [4], which may, for example, be used for multiple-channel wavelength conversion [5].

In addition to providing phase matching, QPM gratings have the basic effect that they induce an asymmetric cubic nonlinearity (ACN) in the equations for the average field in the form of self- and cross-phase modulation terms [6]. This ACN appears in linear and/or nonlinear periodic QPM gratings of arbitrary shape [7], it can be focusing or defocusing, depending on the sign of the phase mismatch [7], and its strength can be increased (e.g., dominating the Kerr nonlinearity) by modulation of the grating [8]. In continuous-wave operation the ACN induces an intensity-dependent phase mismatch, just as the inherent Kerr nonlinearity, with potential use in switching applications [9, 10]. The ACN further explains a wide spectrum of novel fundamental properties of solitons [6, 7, 11] and modulational instability (MI) [12, 13]. Importantly the ACN is a general effect of non-phase-matched wave interaction and as such appear also in homogeneous $\chi^{(2)}$ materials in the cascading limit. In fact, in this case the asymmetric signature of the ACN may be measured as the difference between the properties in upconversion and downconversion, since there is no effective $\chi^{(2)}$ nonlinearity competing with the ACN as in QPM gratings. Such an experiment was recently

reported [14] and thus the ACN has now been confirmed both numerically and experimentally.

In this paper, we present the results of a complete study into the modulational instability of beams in 1+1D QPM waveguides. We find that in general, the MI gain spectrum has a multi-peaked structure of up to three fundamental bands with accompanying overtones. Our previous work [12, 13] concentrated on the structure of the fundamental (long-wave instability) bands at low transverse wavenumbers. These bands are due to MI of the averaged field, and are predicted by averaged equations, provided the effective ACNs are taken into account for the most accurate description. For example, for QPM with a simultaneous linear and nonlinear grating and/or with a nonlinear grating with a dc-value (as with QPM in polymers [2] and semiconductors [3]), the ACNs can suppress these fundamental bands, making plane waves modulationally stable over hundreds of diffraction lengths [12, 13]. Exact Floquet calculations and numerical simulations confirmed the predictions for the low-frequency bands, but also revealed high-frequency bands not predicted by the averaged theory. These gain bands were surmised to be related to the inherent instability in homogeneous (non-phase-matched) $\chi^{(2)}$ media [12, 13]. However, an accurate *analytic* description of the first overtone bands was not derived and the higher overtone bands were not discussed at all.

Here we concentrate on PPLN slab waveguides, which are $\chi^{(2)}$ media with a purely nonlinear QPM grating with no dc-component. Although more-general kinds of grating can be analysed with our method, we choose to focus on the simpler case for clarity. For example, with this simple QPM grating we do not need to take into account the ACN for an accurate description of MI [12, 13], however our analytic method does allow for such cubic nonlinearities to be included. We present the first analytical and numerical description of the complete MI spectrum with all overtones. We show explicitly that the overtone series are caused by MI in the rapidly varying components of the propagating fields, which are in turn induced by the grating. We derive approximate analytic expressions for the positions of the gain bands and compare them with exact Floquet results and direct numerical simulation, to find good agreement.

II. METHOD

We consider a linearly polarized electric field propagating in a lossless $\chi^{(2)}$ slab waveguide with a QPM grating under conditions for (the most efficient) first-order QPM and type I SHG. The normalized dynamical equations for the slowly varying envelopes of the fundamental $E_1(x, z)$ and second harmonic (SH) $E_2(x, z)$ take the form

$$i\frac{\partial E_1}{\partial z} + \frac{1}{2}\frac{\partial^2 E_1}{\partial x^2} + \chi(z)E_1^*E_2 \exp(i\beta z) = 0, \quad (1)$$

$$i\frac{\partial E_2}{\partial z} + \frac{1}{4}\frac{\partial^2 E_2}{\partial x^2} + \chi(z)E_1^2 \exp(-i\beta z) = 0, \quad (2)$$

where the asterisk means complex conjugate. The x and z scales have been normalised by x_0 and $z_0=k_1x_0^2$, respectively, and $\beta=(k_2-2k_1)z_0$ is the normalized wave-vector mismatch. The nonlinearity is periodic in z with expansion

$$\chi(z) = \sum_n d_n \exp(in\kappa z), \quad (3)$$

where $d_n=d_n^*$ (χ is real) and the grating wave number κ is defined to be positive. The grating will force the same periodicity in the propagating fields. We therefore expand these also:

$$E_1(x, z) = \sum_n w_n(x, z) \exp(in\kappa z), \quad (4)$$

$$E_2(x, z) = \sum_n v_n(x, z) \exp(in\kappa z - i\tilde{\beta}z), \quad (5)$$

where $\tilde{\beta}=\beta-s\kappa$ is the residual mismatch, with $s=\text{sign}(\beta)$ for first-order QPM. Substituting all expansions into Eqs. (1-2) gives

$$(\hat{L}_1 - n\kappa)w_n + \sum_{l,m} d_{n+m-l-s} w_m^* v_l = 0, \quad (6)$$

$$(\hat{L}_2 - n\kappa)v_n + \sum_{l,m} d_{n-m-l+s} w_m w_l = 0, \quad (7)$$

where $\hat{L}_j = i\partial_z + \partial_x^2/(2j) + (j-1)\tilde{\beta}$. This set of equations has plane-wave solutions of the form $w_n(x, z) = \bar{w}_n \exp(i\Lambda z)$, $v_n(x, z) = \bar{v}_n \exp(2i\Lambda z)$ [12, 13].

To study MI we consider small perturbations of the plane-wave solutions:

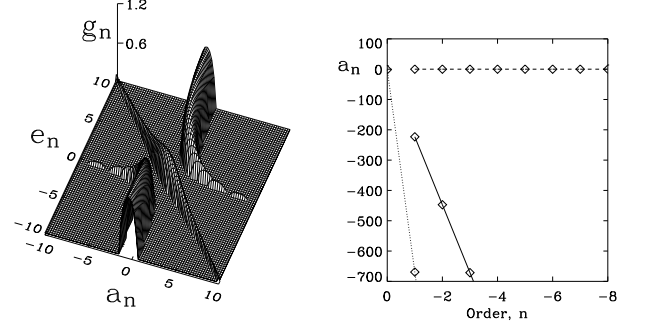


FIG. 1: Left: Maximum gain versus a_n and e_n for $|b_n|^2=1$ and $|c|^2=2$. Right: $a_n(\nu_n)$ for ν_n real and found from Eq. (18) (solid line), from Eq. (19) with plus sign (dotted line), and Eq. (19) with minus sign (dashed line), for $\tilde{\beta}=0$, $\Lambda=1$, and $\kappa=670$.

$$w_n(x, z) = [\bar{w}_n + \epsilon_n(x, z)] \exp(i\Lambda z), \quad (8)$$

$$v_n(x, z) = [\bar{v}_n + \mu_n(x, z)] \exp(2i\Lambda z). \quad (9)$$

Substitution into Eqs. (6-7) gives the linearized equations

$$(\hat{L}'_1 - n\kappa)\epsilon_n + \sum_{l,m} d_{n+m-l-s} (\bar{w}_m^* \mu_l + \bar{v}_l \epsilon_m^*) = 0, \quad (10)$$

$$(\hat{L}'_2 - n\kappa)\mu_n + 2 \sum_{l,m} d_{n-m-l+s} \bar{w}_m \epsilon_l = 0, \quad (11)$$

where $\hat{L}'_j = \hat{L}_j - j\Lambda$. Writing the perturbations in the form

$$\epsilon_n(x, z) = \delta_n^{(1)}(z) \exp(i\nu x) + \delta_n^{(2)*}(z) \exp(-i\nu x) \quad (12)$$

$$\mu_n(x, z) = \delta_n^{(3)}(z) \exp(i\nu x) + \delta_n^{(4)*}(z) \exp(-i\nu x) \quad (13)$$

one obtains a linear matrix equation for the perturbation $\vec{\delta}_n = (\delta_n^{(1)}, \delta_n^{(2)}, \delta_n^{(3)}, \delta_n^{(4)})^T$, which couples all Fourier components.

To derive a simple result we consider nearly phase-matched interaction with $|\kappa| \sim |\beta| \gg 1$ in the typical (for PPLN) square QPM grating, for which $d_n=0$ for n even and $d_n=2/(i\pi n)$ for n odd. The requirement $|\kappa| \sim |\beta| \gg 1$ allows us to assume that the amplitudes w_n and v_n vary slowly compared to $\exp(i\kappa z)$ and that the higher harmonics are much smaller than the dc-fields, $|\bar{w}_0|, |\bar{v}_0| \gg |\bar{w}_{n \neq 0}|, |\bar{v}_{n \neq 0}|$. In this case the structure of

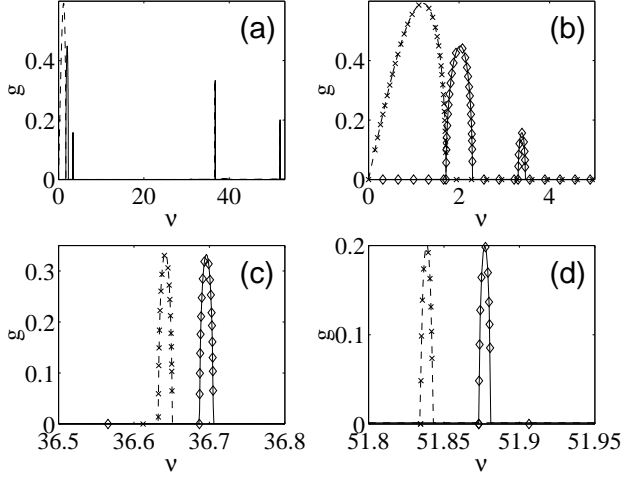


FIG. 2: MI gain for $\Lambda=1$ (dashed) and $\Lambda=-1$ (solid) calculated by Floquet theory. Crosses and diamonds show the theoretical prediction (15). $\kappa=\beta=670$.

the matrix equation means that the evolution of the perturbation in each component is to a good approximation decoupled from the other components,

$$\frac{\partial \vec{\delta}_n}{\partial z} \approx i \begin{bmatrix} a_n & b_n & c & 0 \\ -b_n^* & -a_n & 0 & -c^* \\ 2c^* & 0 & e_n & 0 \\ 0 & -2c & 0 & -e_n \end{bmatrix} \vec{\delta}_n \equiv M_n \vec{\delta}_n, \quad (14)$$

where $a_n = -\nu^2/2 - \Lambda - n\kappa$, $b_n = d_{2n-s}\bar{v}_0$, $c = d_{-s}\bar{w}_0^*$, and $e_n = -\nu^2/4 + \tilde{\beta} - 2\Lambda - n\kappa$. The eigenvalues of M_n are

$$\lambda_n^2 = A_n \pm \sqrt{A_n^2 - B_n}, \quad (15)$$

where

$$A_n = \frac{1}{2}(|b_n|^2 - a_n^2 - 4|c|^2 - e_n^2), \quad (16)$$

$$B_n = (a_n e_n - 2|c|^2)^2 - e_n^2 |b_n|^2. \quad (17)$$

Any positive real part of an eigenvalue corresponds to MI with the gain $g_n(\nu) = \Re(\lambda_n)$.

III. RESULTS

For the gratings that we consider here, $|c|^2 \simeq \Lambda(2\Lambda - \tilde{\beta})$ and $|b_n|^2 \simeq \Lambda^2/(2n-s)^2$. Analysing the gain versus a_n

and e_n reveals three gain bands, with extrema remaining close to $a_n = -e_n$ (diagonal branch DB) and $a_n e_n = 2|c|^2$ (hyperbolic branches HB_+ , HB_-), as illustrated in Fig. 1 for $|b_n|^2 = 1$ and $|c|^2 = 2$. The extrema $a_n = -e_n$ of DB correspond to

$$\nu_n^2 = -8n\kappa/3 - 4\Lambda + 4\tilde{\beta}/3, \quad (18)$$

while the extrema $a_n e_n = 2|c|^2$ of HB_+ and HB_- correspond to

$$\nu_n^2 = 2\tilde{\beta} - 3n\kappa - 5\Lambda \pm \sqrt{(2\tilde{\beta} - n\kappa - 3\Lambda)^2 + 16|c|^2}. \quad (19)$$

For $n \neq 0$ the HB_+ bands appear at $\nu^2 \simeq -4\kappa n - 8\Lambda + 4\tilde{\beta}$ and the HB_- bands at $\nu^2 \simeq -2\kappa n - 2\Lambda$. Thus we have the structure of up to 3 gain bands in the average field ($n=0$), each with a set of equally spaced (in ν^2) weak overtone gain bands ($n \neq 0$). However, the gain is large only near $a_n=0$ (see Fig. 1). For $n \neq 0$, $a_n \simeq 0$ can be satisfied without violating the assumptions only on HB_- , and thus the overtones of the other branches will be small.

Consider a system at exact phase-matching $\tilde{\beta} = 0$, with dimensionless parameters $|\Lambda| = 1$ and $\kappa = 670$. For a LiNbO₃ QPM grating with period $\lambda_g = 17.6\mu\text{m}$ designed to phase-match at wavelengths of around $\lambda = 1550\text{nm}$, these dimensionless parameters correspond to having an input intensity of $I = 6.7\text{GW}/\text{m}^2$, if one assumes a waveguide depth of $y_0 = 3.1\mu\text{m}$. The distance scaling parameters for this case are $x_0 = 21.6\mu\text{m}$ and $z_0 = 1.89\text{mm}$. For fixed distance scaling, different values of the magnitude of Λ correspond to different input intensities, and different signs of Λ correspond to different ratios of the fundamental to second harmonic[13]. On the other hand, keeping $|\Lambda|$ fixed while varying the input intensity corresponds to changing the distance scaling: to a good approximation, $z_0 \propto I^{-1/2}$, $x_0 \propto I^{-1/4}$, and hence $\kappa \propto I^{1/2}$.

For $\Lambda=1$ our analytic results predict only one fundamental $n=0$ gain band (HB_+) and three gain bands in all overtones. However the overtones of DB and HB_+ are too small to be seen. Thus the visible gain bands have maxima at $\nu_0=1.18$ (HB_+), $\nu_{-1}=36.64$, $\nu_{-2}=51.84$, etc. (all HB_-). In physical units these are $\nu_0 = 0.055\mu\text{m}^{-1}$, $\nu_{-1} = 1.697\mu\text{m}^{-1}$, and $\nu_{-2} = 2.401\mu\text{m}^{-1}$, respectively. The analytical results agree with exact Floquet calculations [12, 13], as seen in Fig. 2.

For $\Lambda=-1$ two fundamental $n=0$ bands are predicted (DB and HB_+), with one set of visible overtones from HB_- . The maxima are at $\nu_0=2$ (DB), $\nu_0=3.38$ (HB_+), $\nu_{-1}=36.70$, $\nu_{-2}=51.88$, etc. (all HB_-). In physical units these are $\nu_0 = 0.093\mu\text{m}^{-1}$, $\nu_0 = 0.0157\mu\text{m}^{-1}$, $\nu_{-1} = 1.700\mu\text{m}^{-1}$, and $\nu_{-2} = 2.403\mu\text{m}^{-1}$, respectively. This is again confirmed by the exact Floquet calculations seen in

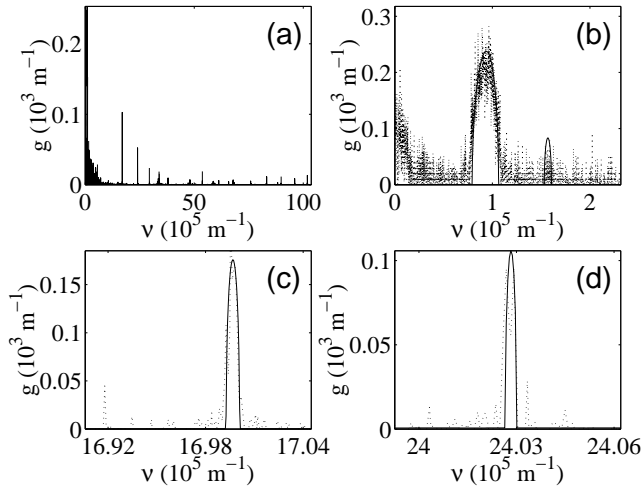


FIG. 3: Gain calculated by numerical simulation [(a) and dotted line in (b-d)] and by Floquet theory [solid line in (b-d)]. $\kappa = \beta = 670$ and $\Lambda = -1$.

Fig. 2. Figure 2 also shows the gain profiles predicted by Eq. (15), which agree well with the exact Floquet results. Direct numerical simulation [12, 13] of Eqs. (1-2) with MI

seeded by noise also confirmed our results (see Fig. 3).

We see from Eqs. (18-19) that the dimensionless spectral positions of the higher-order bands depends on κ , whereas the fundamental bands do not. The different dependence implies a different scaling with input intensity, since for fixed $|\Lambda|$, both the distance scalings x_0 , z_0 and the dimensionless wave vector κ depend on the intensity. The result is that the spatial frequencies of the higher-harmonic instabilities remain the same, in physical units, whereas the frequencies of the fundamental-band instabilities generally increase with the quartic root of the intensity.

IV. SUMMARY

In conclusion, we have presented a simple theory able to accurately predict the complete MI spectrum in general QPM gratings in $\chi^{(2)}$ materials. In particular, we have predicted and verified that overtone gain bands originate from MI in the higher-order Fourier components of the field. This research is supported by the Danish Technical Research Council (Grant No. 26-00-0355) and the Australian Research Council.

-
- [1] M.M. Fejer, in *Beam Shaping and Control with Nonlinear Optics*, eds. F. Kajzar and R. Reinisch, 375–406 (Plenum, New York, 1998).
 - [2] V. Ricci, G.I. Stegeman, and K.P. Chan, “Poling of multilayer polymer films for modal dispersion phase matching of second-harmonic generation: effects in glass-transition temperature matching in different layers”, *J. Opt. Soc. Am. B.* **17**, 1349–1353 (2000).
 - [3] A. Saber Helmy, D.C. Hutchings, T.C. Kleckner, J.H. Marsh, A.C. Bryce, J.M. Arnold, C.R. Stanley, J.S. Aitchison, C.T.A. Brown, K. Moutzouris, and M. Ebrahimzadeh, “Quasi-phase-matching in GAAS-ALAS superlattice waveguides via bandgap tuning using quantum well intermixing”, *Opt. Lett.* **25**, 1370–1372 (2000).
 - [4] P. Baldi, C.G. Trevino-Palacios, G.I. Stegeman, M.P. De Micheli, D.B. Ostrowsky, D. Delacourt, and M. Papuchon, “Simultaneous generation of red, green and blue light in room temperature periodically poled lithium niobate waveguides using single source”, *Electron. Lett.* **31**, 1350–1351 (1995).
 - [5] M.H. Chou, K.R. Parameswaran, M.M. Fejer, and I. Brener, “Multiple-channel wavelength conversion by use of engineered quasi-phase-matching structures in LiNbO₃ waveguides”, *Opt. Lett.* **24**, 1157–1159 (1999).
 - [6] C. Balslev Clausen, O. Bang, and Y.S. Kivshar, “Spatial solitons and induced Kerr effects in quasi-phase-matched quadratic media”, *Phys. Rev. Lett.* **78**, 4749–4752 (1997).
 - [7] J.F. Corney and O. Bang, “Solitons in quadratic nonlinear photonic crystals”, *Phys. Rev. E* **64**, 047601-1–047601-4 (2001).
 - [8] O. Bang, C. Balslev Clausen, P.L. Christiansen, and L. Torner, “Engineering competing nonlinearities”, *Opt. Lett.* **24**, 1413–1415 (1999).
 - [9] O. Bang, T.W. Graversen, and J.F. Corney, “Accurate switching intensities and optimal length scales in quasi-phase-matched materials”, *Opt. Lett.* **26**, 1007–1009 (2001).
 - [10] A. Kobayakov, F. Lederer, O. Bang, and Y.S. Kivshar, “Nonlinear phase shift and all-optical switching in quasi-phase-matched quadratic media”, *Opt. Lett.* **23**, 506–508 (1998).
 - [11] S.K. Johansen, S. Carrasco, L. Torner, and O. Bang, “Engineering of spatial solitons in two-period QPM structures”, *Opt. Commun.* **203**, 393–402 (2002).
 - [12] J.F. Corney and O. Bang, “Modulational instability in periodic quadratic nonlinear materials”, *Phys. Rev. Lett.* **87**, 133901-1–133901-4 (2001);
 - [13] J.F. Corney and O. Bang, “Plane waves in periodic, quadratically nonlinear slab waveguides: stability and exact Fourier structure”, *J. Opt. Soc. Am. B* **19**, 812–821 (2002).
 - [14] P. Di Trapani, A. Bramati, S. Minardi, W. Chinaglia, C. Conti, S. Trillo, J. Kilius, and G. Valiulis, “Focusing versus defocusing nonlinearities due to parametric wave mixing” *Phys. Rev. Lett.* **87**, 183902-1–183902-4 (2001).